Dalton Transactions

PAPER

View Article Online
View Journal

Cite this: DOI: 10.1039/c5dt01407g

Synthesis of a series of new platinum organometallic complexes derived from bidentate Schiff-base ligands and their catalytic activity in the hydrosilylation and dehydrosilylation of styrene†

M. Belhadj Lachachi,[a,b] Tayeb Benabdallah,[b] Pedro M. Aguiar,[a] M. Hadj Youcef,[b] Adrian C. Whitwood[a] and Jason M. Lynam*[a]

Received 14th April 2015,
Accepted 26th May 2015

DOI: 10.1039/c5dt01407g

www.rsc.org/dalton

The synthesis and properties of a novel class of platinum complexes containing Schiff bases as O,N-bidentate ligands is described as are the solution and solid state properties of the uncomplexed ligands. The platinum complexes were prepared from [$PtBr_2$(COD)] (COD = 1,5-cyclooctadiene) and *N*-(2-hydroxy-1-naphthalidene)aniline derivatives in the presence of base ($NaOBu^t$). Instead of a substitution reaction to afford cationic species, the addition of the Schiff base ligands results in both the formal loss of two equivalents of bromide and addition of hydroxide to the COD ligand of the complexes. It is proposed that this reaction proceeds through a cationic platinum complex [Pt(N–O)(COD)]Br which then undergoes addition of water and loss of HBr. An example of a dinuclear platinum complex in which two cyclo–octene ligands are bridged by an ether linkage is also reported. The platinum complexes were evaluated as catalysts for the hydrogenative and dehydrogenative silylation of styrene, the resulting behaviour is substituent, time and temperature dependent.

Introduction

Schiff bases represent a versatile and diverse class of ligands for transition metal compounds. The ligands are typically prepared from the condensation reaction of either an aldehyde or ketone with a primary amine and, as such, it is possible to introduce a wide variety of steric and electronic features into their structure.[1] Traditional Schiff bases act as bidenatate N–O donors to a single metal centre, however, there are additional examples in which the ligand may act as a tridentate N,O,O-, N,O,N-, N,O,S- or tetradentate N,N,O,O-donor ligand permitting the synthesis of multinuclear complexes, including one- two- and three-dimensional metal organic frameworks.[2] Therefore, Schiff base ligands have found widespread application in catalysis,[3] electrochemistry,[4] nanotechnology,[5] materials science[6] and as potential therapeutic agents.[7] Schiff base ligands typically coordinate to transition metals through hard nitrogen and oxygen donors and as such have principally found application with first row and/or early transition metals.[8] However, there are a number of complexes reported in which these ligands bind to softer metals such as ruthenium(II), rhodium(I), palladium(II) and platinum(II).[9]

As expected from their hard nature, Schiff base ligands have found their principal application in oxidation/reductive reactions as well as catalysts for hydrolysis.[10] However, including hard donor ligands into the coordination sphere of soft metal centres raises the possibility of introducing unusual electronic features at a given metal and thus imparting novel catalytic properties when compared to more traditional ligands for low oxidation state metals such as phosphines, alkenes and carbon monoxide. In addition to creating such a hard/soft mismatch, Schiff base ligands are attractive as it is relatively straightforward to prepare a library of related ligands, thus allowing structure/activity relationships to be readily probed.

The synthesis of some new platinum complexes which contain hard Schiff base ligands using [$PtBr_2$(COD)] as a precursor is now described. The coordination of the Schiff base promotes an unusual hydration reaction of the cyclo–octadiene ligand. The new platinum complexes are catalysts for hydrogenative and dehydrogenative silylation of styrene and the

[a]Department of Chemistry, University of York, Heslington, York, YO10 5DD, UK. E-mail: Jason.lynam@york.ac.uk; Tel: +44 (0)1904322534
[b]Laboratory of Chemistry and Electrochemistry of Metallic Complexes, Department of Organic Chemistry, Faculty of Chemistry, University of Sciences and Technology of Oran, BP 1505 El M'Naouar, Oran, 31000, Algeria

†Electronic supplementary information (ESI) available: Details of X-ray diffraction experiments, UV-vis, MS and NMR spectra. CCDC 1055267–1055271. For ESI and crystallographic data in CIF or other electronic format see DOI: 10.1039/c5dt01407g

activity depends upon the nature of the substituents on the Schiff base.

Results and discussion

Five naphthyl-substituted Schiff-base ligands, **3**, were prepared in good yield from the condensation of 2-hydroxy-1-naphthaldehyde, **1**, with 4-substituted anilines **2** (Scheme 1) using the method described by Salman and co-workers.[11] In addition to characterisation by NMR spectroscopy, elemental analysis and mass spectrometry, the structures of **3a** (Fig. 1), **3c** (Fig. 2) and **3d** (Fig. 3) were determined by single crystal X-ray diffraction.

Compounds **3** exhibit a keto–enol tautomerisation[12] (Scheme 2) and the effects of the different substituents present was probed by a number of different techniques. The UV-visible spectra of the organic ligands were studied in a series of solvents with different polarity ranging from protic, polar aprotic to non-polar.[13] The results indicate that the studied Schiff bases are characterized by the presence of two tautomers, a phenol–imine form and a keto–amine form. It was also observed that the Schiff bases show two bands in the visible region located above 400 nm (see ESI†) which were assigned to the keto–amine form.[11] The phenol–imine form has no appreciable absorbance in this region. The UV-visible spectra for the five Schiff base ligands indicates an increase in the proportion of the keto–amine form as the solvent polarity increases. It was concluded that the phenol–imine form predominates in non-polar aprotic solvents such as toluene and cyclohexane, while the keto–amine form is predominant in polar solvents, such as chloroform and ethanol. Indeed, in a related system the keto–amine form has been shown to be highly polar and a charge-density study supports a contribution to the bonding from the proposed Lewis structure.[14]

A comparison between the ^{1}H and ^{13}C NMR spectroscopic data in both solution and solid state is given in Table 1, which are consistent with previous reports.[15] In the ^{13}C CPMAS NMR spectrum the chemical shifts of C-2 and C-α (see Scheme 2 for labelling) are sensitive to the proton position and gives an indication of the relative population of both tautomers. The chemical shift of the C-2 carbon of **3a** (δ 189.9) suggests that the keto–amine form dominates in this structure. The data from a single crystal X-ray diffraction study support this argument with the observation of short C(1)–O(1), 1.2683(14) Å, and long C(11)–N(1), 1.3321(14) Å, bonds. In **3d**, the chemical shift of C-2 in the solid state ^{13}C NMR is δ 172.9 suggesting a

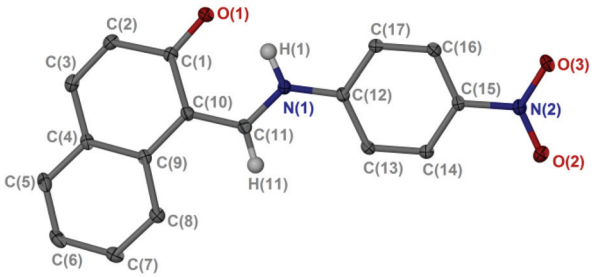

Fig. 1 Solid state structure of **3a**, thermal ellipsoids are shown at the 50% probability level, selected hydrogen atoms removed for clarity. Selected bond lengths (Å) and angles (°) C(1)–O(1) 1.2683(14), C(11)–N(1) 1.3321(14), C(12)–N(1) 1.3922(14), C(15)–N(2) 1.4500(14); N(2)–O(2) 1.2305(13), N(2)–O(3) 1.2289(14); C(11)–N(1)–C(12) 127.54(10), O(1)–C(1)–C(10) 122.69(11).

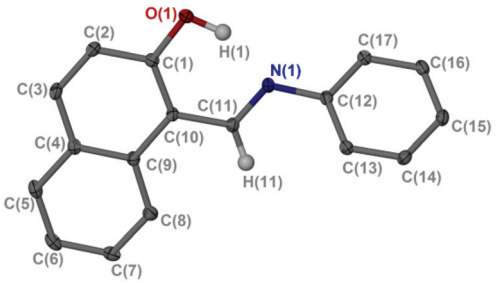

Fig. 2 Solid state structure of **3c**, thermal ellipsoids are shown at the 50% probability level. Selected bond lengths (Å) and angles (°) C(11)–N(1) 1.2932(14), C(12)–N(1) 1.4143(14), C(1)–O(1) 1.3427(16); C(11)–N(1)–C(12) 119.71(10), O(1)–C(1)–C(10) 122.30(10).

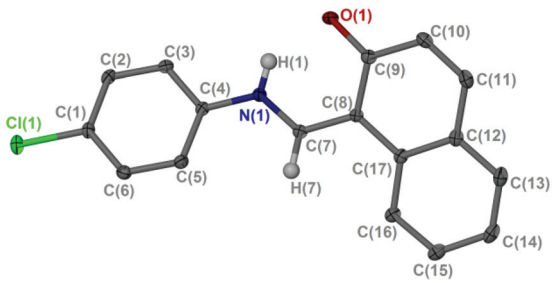

Fig. 3 Solid state structure of **3d**, thermal ellipsoids are shown at the 50% probability level. Selected bond lengths (Å) and angles (°) C(1)–Cl(1) 1.7354(12), C(4)–N1 1.4039(16), C(7)–N(1) 1.3060(16), C(9)–O(1) 1.3026(16); C(7)–N(1)–C(4) 124.16(11), O(1)–C(9)–C(8) 122.14(12).

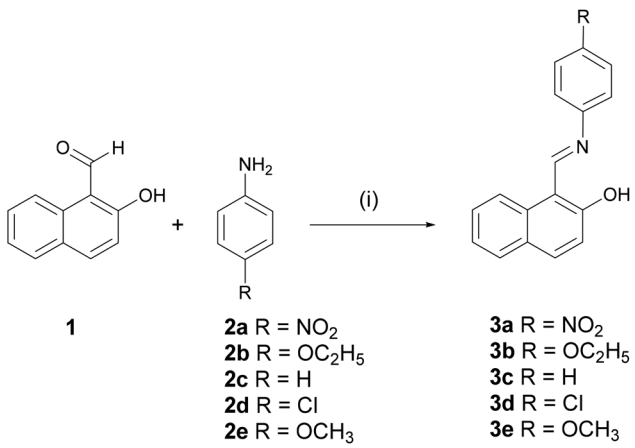

Scheme 1 (i) EtOH, 2 hours, reflux.

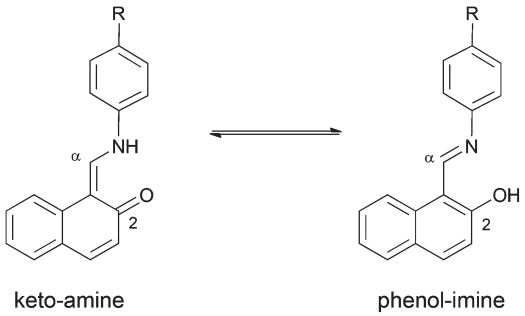

Scheme 2 Keto–enol tautomerisation in compounds **3**.

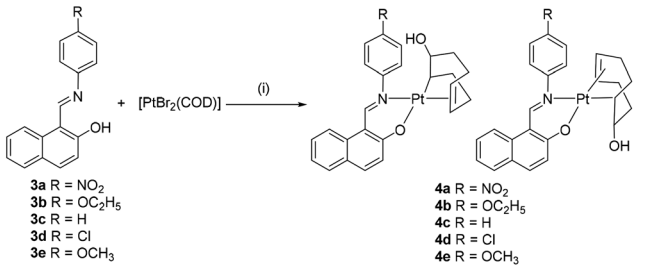

Scheme 3 (i) +NaO^{t}Bu, +H_2O, –NaBr, –HBr, –HO^{t}Bu, thf, 24 h.

Table 1 Comparison between the solution and the solid state NMR for the five bidentate Schiff bases (selected ^{1}H and ^{13}C chemical shifts)

	NH/OH (ppm)		C-2 (ppm)		C-α (ppm)	
Entry	CD_2Cl_2	Solid	CD_2Cl_2	Solid	CD_2Cl_2	Solid
3a	14.88	11.9	193.9/168.8[a]	189.9	158.2	141.7
3b	15.62	16.3	167.8	169.9	154.9	149.5
3c	15.46	14.2	169.4	180	155.5	145.1
3d	15.2	15.2	167.5	172.9	157.3	148.2
3e	15.59	15.2	167.9	170.1	155.2	148.9

[a] Slow exchange between tautomers occuring.

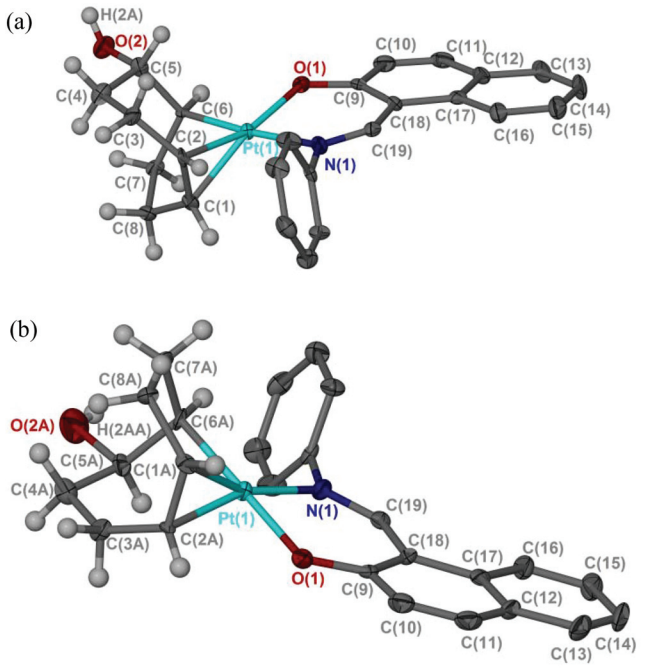

Fig. 4 Solid state structure of **4c** (a) major component (79%) and (b) minor component (21%). Thermal ellipsoids are shown at the 50% probability level, selected hydrogen atoms omitted for clarity. Selected bond lengths (Å) and angles (°) in major form. Pt(1)–N(1) 2.106(4), Pt(1)–O(1) 2.028(4), Pt(1)–C(1) 2.136(7), Pt(1)–C(2) 2.149(7), Pt(1)–C(6) 2.011(6), C(1)–C(2) 1.413(10), C(5)–C(6) 1.540(12), O(2)–C(5) 1.435(12); N(1)–Pt(1)–C(1) 103.1(3), N(1)–Pt(1)–C(2) 95.7(2), O(1)–Pt(1)–N(1) 87.79(15), O(1)–Pt(1)–C(1) 154.9(3), C(6)–Pt(1)–N(1) 175.3(2), C(6)–Pt(1)–O(1) 87.9(2), C(6)–Pt(1)–C(1) 81.5(3), C(6)–Pt(1)–C(2) 88.0(3). Selected bond lengths in minor form (Å) Pt(1)–C(1A) 2.206(17), Pt(1)–C(2A) 2.144(19), Pt(1)–C(6A) 1.982(19).

greater contribution from the phenol–imine form and analysis of the X-ray data of this compound, shows a longer C(9)–O(1) 1.3026(16) and a shorter C(7)–N(1) 1.3060(16) bond. Unfortunately, the correlation between the chemical shift of C-2 in the solid state ^{13}C NMR spectrum and the structure obtained by X-ray diffraction does not hold for **3c**, the latter technique predicts that the phenol–imine form should dominate (C(1)–O(1) 1.3427(16) Å, C(11)–N(1) 1.2932(14) Å), but the resonance of C-2 is actually less-shielded than that for **3d**. However, it should be noted that the two experiments report on the nature of the chemical environment at two very different temperatures, *ca.* 300 K for NMR *versus* 110 K for X-ray. In any event, it is clear that the substituent on the phenyl ring and the solvent has a significant effect on the keto–enol tautomerisation.

In order to explore the coordination chemistry of ligands **3**, a platinum-based precursor was employed. Reaction of [$PtBr_2$(COD)] with ligands **3** in the presence of NaO^{t}Bu resulted in the formation of platinum complexes **4** (Scheme 3). Analysis of the products by ^{1}H NMR spectroscopy revealed that two products in approximately a 3.5 : 1 ratio were present, each with an imine proton that exhibited platinum satellites, confirming that the Schiff base ligand was coordinated to the metal. Evidence for a coordinated C_8 ligand was also present, although the number of resonances indicated that the complexes did not contain a mirror plane.

The identity of complexes **4** was confirmed by a single crystal X-ray diffraction study on **4c** (Fig. 4). This study demonstrated that the Schiff-base ligand was coordinated to the platinum through its nitrogen and oxygen atoms. However, the structure determination demonstrated that the COD ligand had been functionalised when compared to the precursor and an extra peak of electron density was present which was modelled as a hydroxyl group. The hydroxyl was disordered over two positions and thus explained the appearance in the NMR spectra of two imine resonances which were assigned to the two geometric isomers of **4**. The bond lengths between the platinum and the three metal bound carbons are consistent

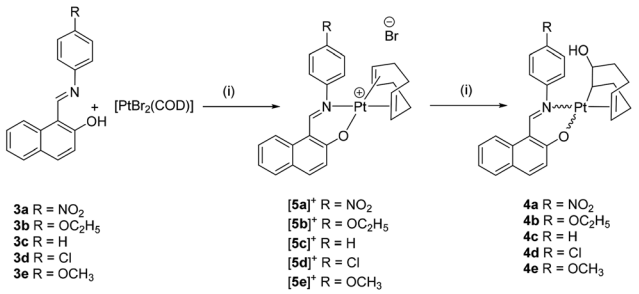

Scheme 4 (i) $+NaO^tBu$, $-NaBr$ $-HO^tBu$, (ii) $+H_2O$, $-HBr$, thf, 24 h.

with C(1) (2.136(7) Å), and C(2) (2.149(7) Å) binding as a π-bound alkene, whereas C(6) (2.011(6) Å) is a typical platinum–carbon single bond.

A possible pathway explaining the formation of complexes **4** is shown in Scheme 4. It is proposed that NaO^tBu acts to deprotonate the –OH group of **3** which then reacts with $[PtBr_2(COD)]$ to give cationic intermediate $[\mathbf{5}]^+$. Nucleophilic attack of adventitious water onto the coordinated COD ligand will then be enhanced by the cationic nature of $[\mathbf{5}]^+$. Formal loss of HBr will then afford the observed product. Furthermore, attempts to record mass spectra of complexes **4** exhibited a peak with a mass-to-charge ratio corresponding to $[\mathbf{5}]^+$. This may indicate that (at least in the mass spectrometer) loss of OH^- from **4** may occur.

Nucleophilic attack at COD ligands within the coordination sphere of both neutral[16] and cationic[17] d^8-metal complexes is a well-established process. Attack at neutral complexes with alkoxide or malonate-based nucleophilies occurs directly at the COD ligand, whereas in the case of Grignard reagents an initial M–C bond formation is followed by migration of the organic group to COD.[16d] Given that water is much poorer nucleophile that many of those previously studied, we favour a pathway involving the cationic intermediate with the *exo* attack indicated in the structure of **4c** indicating that direct addition to the COD has occurred.[16d]

On one occasion a further complex was obtained from an attempt to re-crystallise complex **4e**. In this instance, a single crystal X-ray diffraction study demonstrated that a dimeric species was obtained in which two complexes are bridged by a single oxygen atom (Fig. 5).

The structural determination demonstrated that each platinum was in an approximately square-planar environment and that in the case of Pt(1) the nitrogen atom was *trans* to the alkyl-part of the modified COD ligands and the oxygen *trans* to the carbon–carbon double bond. At Pt(2) the relative position of the nitrogen and oxygen atoms with respect to the organic ligand are interchanged. The bond metrics within the coordination environment of each platinum reflect these changes, for example, when the heteroatom is *trans* to the hard alkyl group the Pt–X bonds are lengthened, whereas the metal–heteroatom bonds are shortened when *trans to* the softer, π-accepting, alkene group. The formation of **6e** may be explained on the basis of the initial mechanistic hypothesis.

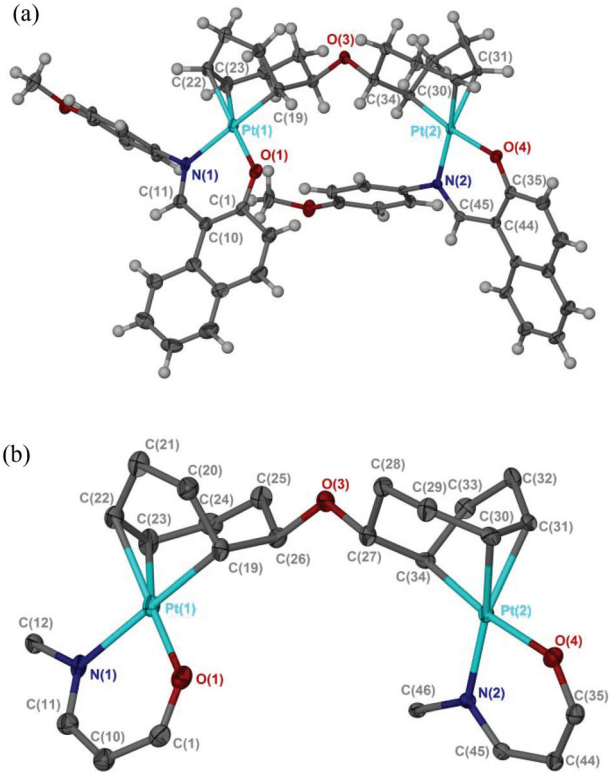

Fig. 5 (a) Solid state structure of **6e**, pentane of crystallisation omitted for clarity (b) coordination environment of the two platinum atoms. Thermal ellipsoids are shown at the 50% probability level, selected hydrogen atoms omitted for clarity. Selected bond lengths (Å) and angles (°) N(1)–Pt(1) 2.116(4), N(2)–Pt(2) 2.051(4), O(1)–Pt(1) 2.017(4), O(4)–Pt(2) 2.091(3), C(22)–Pt(1) 2.103(5), C(23)–C(24) 1.474(7), C(23)–Pt(1) 2.120(5), C(19)–Pt(1) 2.048(4), C(30)–Pt(2) 2.148(4), C(31)–C(32) 1.504(7), C(31)–Pt(2) 2.133(4), C(26)–O(3) 1.429(5), C(27)–O(3) 1.446(5), C(34)–Pt(2) 2.058(4); O(1)–Pt(1)–N(1) 88.43(15), N(2)–Pt(2)–O(4) 89.09(13), C(19)–Pt(1)–N(1) 175.69(17), C(34)–Pt(2)–O(4) 173.07(15).

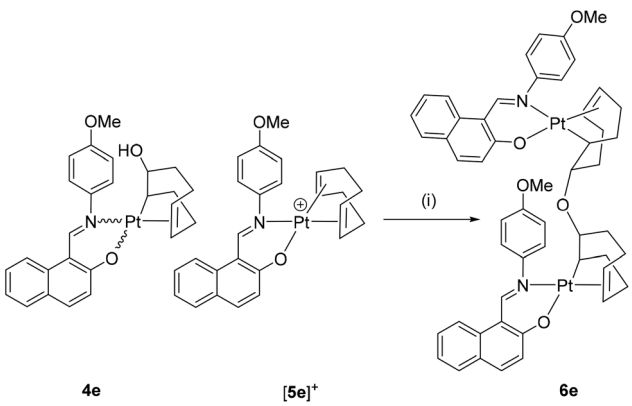

Scheme 5 (i) thf, $-H^+$.

Here, the hydroxyl-group of a complex **4e** undergoes a further reaction with putative **5** to give **6e** (Scheme 5). Alternatively, complexes **6** could be formed from the dehydration of two equivalents of **4**. In any event, the *exo* attack indicated in the

structure of **6e** indicates that direct combination of the COD ligands is occurring.

The ability of the platinum complexes to promote hydrosilylation was then explored. The formation of Si–C bonds remains a key industrial process and platinum-based systems, such as Speier's and Karstedt's catalysts played an important role in the development of transition metal mediated hydrosilylation.[18] More recently a number of other metal-based systems have been shown to be active catalysts.[19] Furthermore, there are number of different competing pathways in a given hydrosilylation reaction, including different regiochemical outcomes and processes such as dehydrosilylation.[20] Access to a number of related catalyst structures with various different functional groups would allow for the effects of these substituents on the outcome of the reaction to be readily probed.

Our experiments focused on the ability of complexes **4** to promote the addition of $HSiEt_3$, **8**, to styrene, **7**. When the resulting reaction was monitored by GC-MS it was clear that in addition to hydrosilylation occurring to give **9** (Scheme 6), dehydrosilylation was competing to give **10**. With this in mind, the effects of a number of variables in the reaction such as the nature of the catalyst, time and temperature on the outcome of the reaction were explored. In order to achieve this, a number of reactions were performed in NMR tubes using d^8-toluene as solvent, 5 mol% of platinum catalyst[21] and a 1 : 1 ratio of **7** to **8**. In addition to ^{1}H NMR, reaction progress was monitored by gas chromatography (GC), following the conversion of **7** to products.

The data in Table 2 illustrate the conversion rate for the hydrosilylation of styrene by triethysilane after 12 h, with different catalyst precursors and temperature variation from 50 °C to 110 °C. It is clear that both of the catalysts **4b** and **4e** have a better catalytic activity than the other platinum complexes, except at 70 °C, where **4c** and **4e** have the highest activity. In general, the activity of the catalysts may be divided into two groups, the first containing electron withdrawing groups, **4a** and **4d**, the other electron donatings groups, **4b** and **4e**, with **4c** is situated in the middle.

The catalytic data demonstrate that at 110 °C all of the platinum complexes give excellent conversion to hydrosilylated products. The ratio of **9** to **10** varies depending on both the

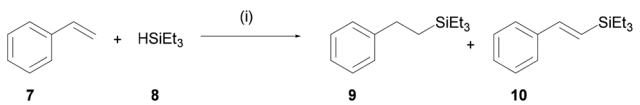

Scheme 6 (i) toluene, 12 h, **4** (5 mol%).

Table 2 Total conversions/% for hydrosilylation reaction of $HSiEt_3$ and styrene (formation of **9**) in the presence of **4a–e** at different temperatures[a]

	Temp. (°C)			
Catalyst	50	70	90	110
4a	30	38	32	50
4b	42	35	49	65
4c	36	46	45	46
4d	35	31	33	42
4e	37	43	45	60

[a] Reaction conditions: $HSiEt_3$ (**8**) (0.18 mmol), styrene (**7**) (0.18 mmol), **4a–e** (5 mol%), toluene (0.5 mL), 12 h. Product yields calculated by ^{1}H NMR and verified by GC-MS (conversion relative to concentration of $HSiEt_3$).

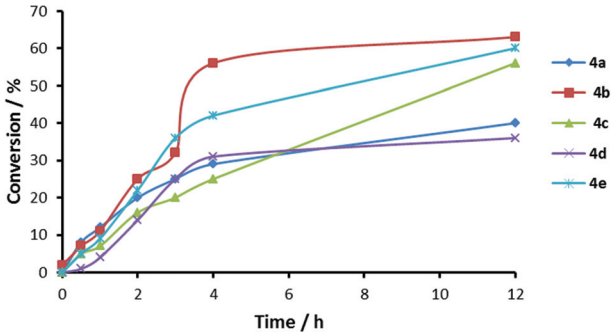

Fig. 6 Catalyst activity over 12 h of complexes **4a–4e** in the reaction between $HSiEt_3$ and styrene showing the formation of the **9** at 110 °C. The lines shown are a guide to the eye.

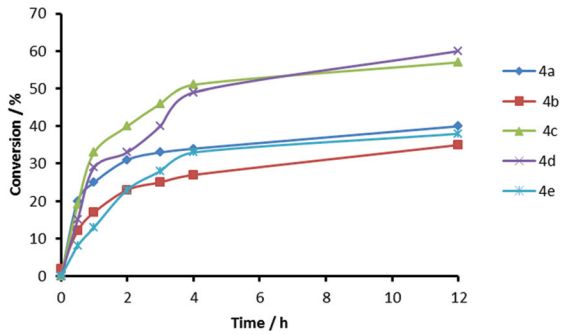

Fig. 7 Catalyst activity over 12 h of the complexes **4a–4e** for the formation of **10** from styrene and $HSiEt_3$ at 110 °C. The lines shown are a guide to the eye.

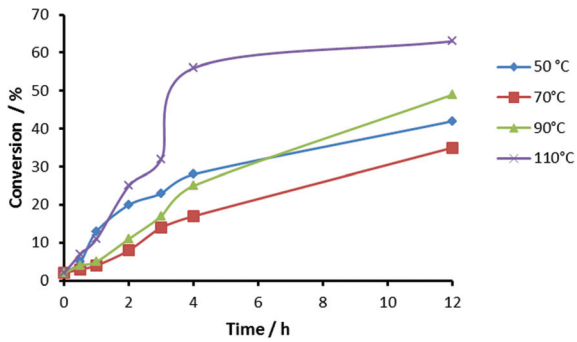

Fig. 8 Catalytic activity for complex **4b** in the hydrosilylation of styrene by $HSiEt_3$ at different temperatures over 12 h. The lines shown are a guide to the eye.

Table 3 Conversions/% to the hydrosilated **9** and the dehydrosilylated product **10** by varying the time and the catalyst during the reaction of $HSiEt_3$ with styrene[a]

Time	1 h		2 h		3 h		4 h		12 h	
Product	**9**[b]	**10**[b]	**9**[b]	**10**[b]	**9**[b]	**10**[b]	**9**[b]	**10**[b]	**9**[b]	**10**[b]
Catalyst										
4a	12	25	20	31	25	32	29	34	50	50
4b	11	17	25	23	32	24	56	26	65	35
4c	7	33	16	40	20	46	25	51	46	54
4d	4	29	14	35	25	41	31	48	42	58
4e	9	13	22	23	36	28	42	33	60	40

[a] Reaction conditions: $HSiEt_3$ (**6**) (0.18 mmol), styrene (**5**) (0.18 mmol), **4a–e** (5 mol%), toluene (0.5 mL) at 110 °C. [b] Product yields calculated by ^{1}H NMR and verified by GC-MS.

reaction time and the nature of the catalyst (Fig. 6–8, Table 3). In all cases, the greatest difference in the ratio of **9** to **10** was observed at short reaction times with **10** dominating under these conditions. Over time the relative proportion of **9** increases in all cases with catalyst **4b** favouring **9** (65%) and **4d** favouring **10** (58%).

At this stage it is not clear what precise influence the substituent on the ligand is having on the catalytic cycle or indeed if it is simply controlling the release of different catalytically-active metal species. For example, the ligand effect may be due to either a traditional structure–activity relationship influencing the relative rates with a homogenous catalytic cycle. Alternatively (or additionally) the nature of the ligand might be controlling the formation of the rate, extent and nature of catalytically active nanoparticles.[22] On the basis of the catalytic data it is evident that the substituent on the ligand has an effect on both the efficiency and selectivity of the reaction.

Conclusions

The incorporation of Schiff-bases based on the *N*-(2-hydroxy-1-naphthalidene)aniline framework into the coordination sphere of platinum may be readily achieved, even when a range of different functional groups are present on the ligand. Coordination of these ligands appears to promote nucleophilic attack by water onto a coordinated COD ligand, presumably *via* a cationic intermediate. The complexes are competent catalysts for the hydrosilylation of styrene and the nature of the ligand affects both the rate of the reaction and the distribution of products between hydrosilyation and dehydrosilyation.

Experimental

All experimental procedures were performed under an atmosphere of dinitrogen using standard Schlenk Line and Glove Box techniques. Dichloromethane, acetonitrile, pentane and hexane were purified with the aid of an Innovative Technologies anhydrous solvent engineering system. Diethyl ether was dried over sodium and CD_2Cl_2 used for NMR experiments was dried over CaH_2 and degassed with three freeze–pump–thaw cycles. The solvent was then vacuum transferred into NMR tubes fitted with PTFE J. Young's taps. All other solvents were used as received from Sigma-Aldrich UK. NMR spectra were acquired on either a Jeol 400 (Operating Frequencies ^{1}H 399.8 MHz, ^{13}C 100.5 MHz) or a Bruker Avance 500 spectrometer (^{1}H 500.2 MHz, ^{13}C 125.8 MHz) at 295 K. ^{13}C spectra were recorded with proton decoupling. In some cases, the resonances for the coordinated COD ligands were complex multiplets that could not be assigned with certainty. Solid state NMR spectra were acquired using a Bruker 4 mm HXY MAS probe on an AvanceIII HD 400 spectrometer equipped with a shielded widebore 9.4 T magnet. All spectra were acquired at a set temperature of 285 K, which corresponds to sample temps of *ca*. 298–300 K at the spinning rates employed. ^{1}H MAS spectra (400.3 MHz) were acquired at 14 kHz spinning rates using a Bloch decay experiment (1 μs, 30 degree pulse), a recycle delay of 20 s and are the sum of 8 co-added transients. Chemical shifts are reported with respect to TMS and were calibrated using adamantane as an external secondary reference (δ = 1.8 ppm). ^{13}C{1H} CPMAS echo spectra (100.6 MHz) were acquired at 12.5 kHz spinning rates with and without a dipolar-dephasing period (450 μs) and employing a ^{1}H flip-back pulse. Experiments employed a 1.5 ms contact pulse (linearly-ramped on ^{1}H), recycle delay of 30–60 seconds, spinal-64 heteronuclear decoupling (at υ_{rf} = 85 kHz) and consist of 64–448 co-added transients. Chemical shifts are reported with respect to TMS, and were referenced using adamantane ($\delta(CH_2)$ = 29.5 ppm) as an external secondary reference. High resolution mass spectrometry was performed by the University of York mass spectrometry service using the ESI technique on a Thermo-Electron Corp LCQ Classic (ESI) instrument or Waters GCT Premier Acceleration TOF MS (LIFDI). IR spectra were acquired on a Thermo-Nicolet Avatar 370 FTIR spectrometer using either CsCl solution cells or as KBr discs. CHN measurements were performed using an Exeter Analytical Inc. CE-440 analyser. Single Crystal X-ray diffraction was carried out on an Oxford Diffraction SuperNova diffractometer with Mo-Kα radiation (λ = 0.71073 Å) using an EOS CCD camera. The crystal was cooled with an Oxford Instruments Cryojet and were kept at 110.00(10) K during data collection. Using Olex2,[23] the structures were solved with the Superflip[24] structure solution program using Charge Flipping except for **3a** which was solved by direct methods[20] and refined with the ShelXL[25] refinement package using least squares minimisation.

Preparation of the bidentate Schiff base ligands

The *N*-(2-hydroxy-1-naphthalidene) *para*-substituted anilines ligands were prepared following the literature,[11] by addition of equimolar quantities of the amine (aniline) in ethanol to a warm solution of 2-hydroxy-1-naphtaldehyde in ethanol and the mixture was heated at reflux for two hours. After cooling, the precipitated products were collected, recrystallized twice

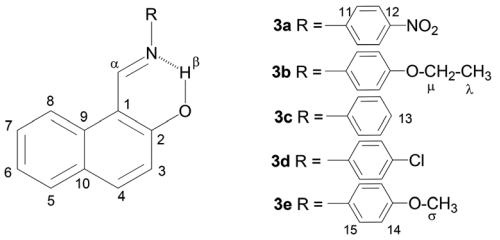

Fig. 9 Structure and molecule numbering of the bidentate Schiff bases derived from 2-hydroxy-1-naphtaldehyde and *p*-substituted anilines.

from ethanol and dried at 25 °C. They were obtained in a yield approaching 80%. Labelling scheme is shown in Fig. 9.

3a ^{1}H NMR (CD_2Cl_2, 399.8 MHz, 293 K): 7.15 (d, 1H, 9.2 Hz, **3**), 7.41 (t, 1H, 7.6 Hz, **6**), 7.16 (d, 2H, 9.1 Hz, **11**, **15**), 7.59 (t, 1H, 7.8 Hz, **7**), 7.78 (dd, 1H, 7.8 Hz, **5**), 7.90 (d, 1H, 9.2 Hz, **4**), 8.18 (d, 1H, 8.2 Hz, **8**), 8.33 (d, 2H, 9.2 Hz, **12**, **14**), 9.45 (d, 1H, 2.5 Hz, **α**), 14.89 (d, 1H, 2.6 Hz, **β**). $^{13}C\{^1H\}$ NMR: (CD_2Cl_2) δ 119.1 (**8**), 121.2 (**3**), 124.6 (**11**, **15**), 125.4 (**6**), 126.3 (**12**, **14**), 129.2 (**7**), 129.6 (**5**), 139.2 (**4**), 158.2 (**α**), 193.9 (**2**). ESI-MS, positive ion: *m*/*z* 293.0918 (calculated for $C_{17}H_{13}N_2O_3$ = 93.0921, Δ = 0.2 mDa); elemental analysis: for $C_{17}H_{12}N_2O_3$ Calc. C 69.86; H 4.14; N 9.58; rest 16.42% Found C 69.88; H 4.38; N 9.56; rest 16.18%; IR (KBr)/cm^{-1} 1621 (C═N), 3431 (X–H)-(X = O; N), 1289 (C–O phenolic).

3b ^{1}H NMR (CD_2Cl_2, 399.8 MHz, 293 K): 1.42 (t, 3H, 7.0 Hz, **λ**), 4.06 (q, 2H, 7.0 Hz, **μ**), 6.98 (d, 2H, 9.0 Hz, **11**, **15**), 7.10 (d, 1H, 9.2 Hz, **3**), 7.35 (td, 1H, 7.5 Hz, **6**), 7.37 (d, 2H, 9.0 Hz, **12**, **14**), 7.54 (t, 1H, 7.7 Hz, **7**), 7.75 (dd, 1H, 7.8 Hz, **5**), 7.81 (d, 1H, 9.1 Hz, **4**), 8.17 (d, 1H, 8.3 Hz, **8**), 9.4 (d, 1H, 3.0 Hz, **α**), 15.64 (d, 1H, 3.1 Hz, **β**). $^{13}C\{^1H\}$ NMR: (CD_2Cl_2) δ 15.0 (**λ**), 64.2 (**μ**), 119.4 (**8**), 121.7 (**3**), 122.1 (**12**, **14**), 123.7 (**6**), 128.2 (**7**), 129.6 (**5**), 135.8 (**4**), 154.9 (**α**), 167.8 (**2**); ESI-MS, positive ion: *m*/*z* 292.1318 (calculated for $C_{19}H_{18}NO_2$ = 292.1332, Δ = 1.4 mDa); elemental analysis: for $C_{19}H_{17}NO_2$ Calc. C 78.33; H 5.88; N 4.81; rest 10.98% Found C 78.17; H 5.83; N 4.73; rest 11.27%; IR (KBr)/cm^{-1} 1616 (C═N), 3430 (X–H)(X = O; N), 1248 (C–O phenolic).

3c ^{1}H NMR (CD_2Cl_2, 399.8 MHz, 293 K): 7.08 (d, 1H, 9.2 Hz, **3**), 7.31 (tt, 1H, 7.4 Hz, **13**), 7.36 (td, 1H, 7.7 Hz, **6**), 7.41 (dd, 2H, 7.9 Hz, **11**, **15**), 7.49 (t, 2H, 7.9 Hz, **12**, **14**), 7.55 (td, 1H, 7.7 Hz, **7**), 7.75 (dd, 1H, 8.2 Hz, **5**), 7.84 (d, 1H, 9.2 Hz, **4**), 8.17 (d, 1H, 8.3 Hz, **8**), 9.42 (s, 1H, **α**), 15.46 (s, 1H, **β**). $^{13}C\{^1H\}$ NMR: (CD_2Cl_2) δ 119.1 (**8**), 120.5 (**11**, **15**), 121.9 (**3**), 123.6 (**6**), 126.6 (**13**), 128.2 (**7**), 129.7 (**5**), 133.3 (**12**, **14**), 136.5 (**4**), 155.5 (**α**), 169.4 (**2**). ESI-MS, positive ion: *m*/*z* 248.1062 (calculated for $C_{17}H_{14}NO$ = 248.1070, Δ = 0.8 mDa); elemental analysis: for $C_{17}H_{13}NO$ Calc. C 82.57; H 5.30; N 5.66; rest 6.47% Found C 82.42; H 5.39; N 5.13; rest 7.06%; IR (KBr)/cm^{-1} 1621 (C═N), 3409 (X–H)(X = O; N), 1179 (C–O phenolic).

3d ^{1}H NMR (CD_2Cl_2, 399.8 MHz, 293 K): 7.12 (d, 1H, 9.1 Hz, **3**), 7.35 (d, 2H, 8.9 Hz, **11**, **15**), 7.38 (t, 1H, 7.7 Hz, **6**), 7.45 (d, 2H, 9.0 Hz, **12**, **14**), 7.56 (t, 1H, 7.8 Hz, **7**), 7.77(dt, 1H, 8.0 Hz, **5**), 7.86 (d, 1H, 9.1 Hz, **4**), 8.17 (d, 1H, 8.2 Hz, **8**), 9.43 (d, 1H, 2.7 Hz, **α**), 15.22 (d, 1H, 2.7 Hz, **β**). $^{13}C\{^1H\}$ NMR: (CD_2Cl_2) δ 119.4 (**8**), 121.3 (**3**), 122.4 (**11**, **15**), 124.0 (**6**), 128.5 (**7**), 129.9 (**5**), 132.2 (**12**, **14**), 136.5 (**4**), 157.3 (**α**), 167.5 (**2**); ESI-MS, positive ion: *m*/*z* 282.0674 (calculated for $C_{17}H_{13}ClNO$ = 282.0680, Δ = 0.6 mDa); elemental analysis: for $C_{17}H_{12}NOCl$ Calc. C 72.47; H 4.29; N 4.97; rest 18.26% Found C 72.32; H 4.25; N 4.88; rest 18.55% IR (KBr)/cm^{-1} 1618 (C═N), 3507 (X–H)(X = O; N), 1181 (C–O phenolic).

3e ^{1}H NMR (CD_2Cl_2, 399.8 MHz, 293 K): 3.85 (s, 3H, **σ**), 7.01 (d, 2H, 9.0 Hz, **11**, **15**), 7.10 (d, 1H, 9.1 Hz, **3**), 7.36 (td, 1H, 7.7 Hz, **6**), 7.39 (d, 2H, 9.0 Hz, **12**, **14**), 7.54 (t, 1H, 7.8 Hz, **7**), 7.76 (dt, 1H, 8.0 Hz, **5**), 7.82 (d, 1H, 9.2 Hz, **4**), 8.18 (d, 1H, 8.3 Hz, **8**), 9.42 (d, 1H, 2.8 Hz, **α**), 15.62 (d, 1H, 3.1 Hz, **β**); $^{13}C\{^1H\}$ NMR: (CD_2Cl_2) δ 56.1 (**σ**), 119.5 (**8**), 121.3 (**3**), 122.3 (**11**, **15**), 124.1 (**6**), 128.5 (**7**), 130.0 (**5**), 133.5 (**12**, **14**), 136.5 (**4**), 155.2 (**α**), 167.9 (**2**); ESI-MS, positive ion: *m*/*z* 278.1165 (calculated for $C_{18}H_{16}NO_2$ = 278.1176, Δ = 1.1 mDa); elemental analysis: for $C_{18}H_{15}NO_2$ Calc. C 77.96; H 5.45; N 5.05; rest 11.54% Found C 77.71; H 5.41; N 4.97; rest 11.91%; IR (KBr)/cm^{-1} 1620 (C═N), 3488 (X–H)(X = O; N), 1246 (C–O phenolic).

Synthesis of dibromo(1,5-cyclooctadiene)platinum(II)

Dibromo(1,5-cyclooctadiene)platinum(II) (2.16 g, 4.6 mmol, 95% yield) was obtained as green crystals from potassium tetrabromoplatinate (2.5 g, 6.0 mmol), glacial acetic acid (60 mL) and 1,5-cyclooctadiene (2.5 mL, 20 mmol) in distilled water (40 ml). The reaction mixture was stirred and heated to about 90 °C over 30 min. The deep red solution slowly became pale yellow and fine crystals were deposited, washed in 50 ml portions of water, ethanol and ether and then dried at 100 °C for 60 min. Labelling scheme is shown in Fig. 10.[26]

Synthesis of 4a. Dibromo(1,5-cyclooctadiene)platinum(II) (50 mg, 0.11 mmol), *N*-(2-hydroxy-1-naphthalidene)-*p*-nitroaniline (31 mg, 0.11 mmol) and sodium *tert*-butoxide (24 mg, 0.22 mmol) were stirred in THF (30 ml) for 16 hours under a nitrogen atmosphere. The solution was then filtered under nitrogen, and the filtrate dried under vacuum for 4 hours. Complex **4a** was obtained as red crystals (70 mg, 0.13 mmol, 60% yield).

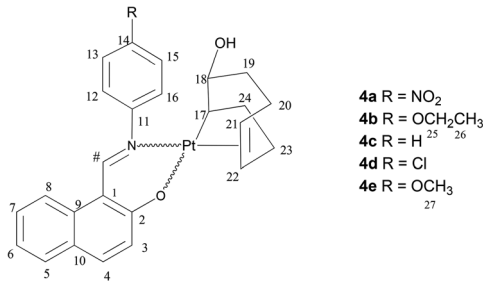

4

Fig. 10 Structure and molecule numbering of the platinum(II) organometallic complexes derived from 2-hydroxy-1-naphthaldehyde and 1,5-cyclooctadiene.

4a**-major isomer.* ^{1}H NMR (CD_2Cl_2, 399.8 MHz, 293 K): δ_H 1.81 (m, 2H), 5.02 (m, 2H, **21** or **22**), 6.91 (d, 1H, 9.6 Hz, **3**), 7.10 (d, 1H, 9.2 Hz, **6**), 7.35 (dd, 2H, 8.3 Hz, **12**, **16**), 7.46 (dd, 2H, 8.6 Hz, **13**, **15**), 7.64 (td, 1H, 7.8 Hz, **7**), 7.72 (d, 1H, 8.2 Hz, **5**); 7.84 (d, 1H, 9.1 Hz, **4**), 8.13 (d, 1H, 8.7 Hz, **8**), 9.02 (s, 1H, $^3J_{Pt-H}$ = 76.2 Hz, Pt–N=CH***). $^{13}C\{^1H\}$ NMR: (CD_2Cl_2) δ 26.1 (**19**), 28.6 (**20**), 31.5 (**23**), 32.4 (**24**), 68.2 (**17**), 73.8 (**18**), 75.8 (**21**, **22**), 111.9 (**1**), 119.3 (**8**), 123.5 (**3**), 124.3 (**6**), 124.9 (**13**, **15**), 126.0 (**9**), 126.9 (**12**, **16**), 127.8 (**14**), 128.6 (**7**), 129.1 (**5**), 135.3 (**10**), 138.4 (**4**), 140.3 (**11**), 153.2 (**#**), 169.7 (**2**).

***4a**-minor isomer.* ^{1}H NMR (CD_2Cl_2, 399.8 MHz, 293 K): 9.21 (s, 1H, $^3J_{Pt-H}$ = 25.4 Hz, Pt–N=CH).

ESI-MS, positive ion: *m*/*z* 594.1329 (calculated for $C_{25}H_{23}N_2O_3Pt$ [M]–O = 594.1353, Δ = 2.2 mDa); elemental analysis: for $C_{25}H_{24}N_2O_4Pt$ calc. C 49.10, H 3.96, N 4.58, rest 42.36%, found C 49.45; H 3.99; N 4.84, rest 41.72% IR (KBr)/cm^{-1} 1579 (C=N), 3431 (O–H), 1262 (C–O phenolic).

Synthesis of 4b. Dibromo(1,5-cyclooctadiene)platinum(II) (100 mg, 0.22 mmol), *N*-(2-hydroxy-1-naphthalidene)-*p*-ethoxyaniline (63 mg, 0.22 mmol) and sodium *tert*-butoxide (50 mg, 0.43 mmol) were stirred in THF (30 ml). The reaction mixture was left in a Schlenk tube under nitrogen and stirring overnight. The solution was then filtered under nitrogen, and dried under vacuum for 4 hours. The complex **4b** was obtained as yellow crystals (70 mg, 0.13 mmol, 60% yield).

***4b**-major isomer.* ^{1}H NMR (CD_2Cl_2, 399.8 MHz, 293 K): 1.43 (t, 3H, 7.0 Hz, **26**), 2.22 (m, 1H), 2.43 (m, 2H), 2.70 (m, 2H), 3.61 (m, 1H), 4.08 (q, 2H, 7.2 Hz, **25**), 4.96 (m, 2H, **21** and **22**), 6.88 (t, 2H, 7.2 Hz, **12**, **16**), 7.13 (d, 1H, 8.7 Hz, **3**), 7.22 (td, 1H, 8.3 Hz, **6**), 7.48 (m, 1H, 7.6 Hz, **7**), 7.87 (d, 1H, 8.7 Hz, **5**), 7.97 (d, 1H, 8.6 Hz, **4**), 8.11 (d, 1H, 9.5 Hz, **8**), 9.05 (s, 1H, $^3J_{Pt-H}$ = 77.8 Hz, Pt–N=CH). $^{13}C\{^1H\}$ NMR: (CD_2Cl_2) δ 15.1 (**26**), 26.0 (**19**), 27.5 (**20**), 28.6 (**23**), 31.5 (**24**), 64.3 (**25**), 68.3 (**17**), 73.9 (**18**), 84.6 (**21**, **22**), 109.3 (**1**), 114.4 (**12**, **16**), 119.4 (**8**), 121.6 (**3**), 125.3 (**6**), 126.9 (**13**, **15**), 127.7 (**9**), 128.3 (**7**), 129.1 (**10**), 129.7 (**5**), 135.8 (**4**), 137.0 (**11**), 155.0 (**14**), 157.8 (**#**), 195.5 (**2**).

***4b**-minor isomer.* ^{1}H NMR (CD_2Cl_2, 399.8 MHz, 293 K): 9.24 (s, 1H, $^3J_{Pt-H}$ = 25.8 Hz, Pt–N=CH).

ESI-MS, positive ion: *m*/*z* 593.1767 (calculated for $C_{27}H_{28}NO_2Pt$ [M]–OH = 593.1765, Δ = −0.2 mDa); elemental analysis: for $C_{27}H_{29}NO_3Pt$ Calc. C 53.11; H 4.79; N 2.29; rest 39.81% Found C 53.57; H 4.81; N 2.75; rest 38.87% IR (KBr)/cm^{-1} 1580 (C=N), 3433 (O–H), 1427 (C–O ether aromatic), 1261 (C–O phenolic).

Synthesis of 4c. Dibromo(1,5-cyclooctadiene)platinum(II) (50 mg, 0.11 mmol), *N*-(2-hydroxy-1-naphthalidene)aniline (26 mg, 0.11 mmol) and sodium *tert*-butoxide (10 mg, 0.22 mmol) were stirred in THF (30 ml). The reaction mixture was left in a Schlenk tube under nitrogen and stirring overnight. The solution was then filtered under nitrogen, and dried under vacuum for 4 hours. The complex **4c** was obtained as yellow crystals (70 mg, 0.13 mmol, 60% yield).

***4c**-major isomer.* ^{1}H NMR (CD_2Cl_2, 399.8 MHz, 293 K): δ_H 1.69 (m, 2H), 3.84 (m, 1H), 4.08 (td, 1H, 8.8 Hz), 4.98 (m, 2H, **21** and **22**), 6.92 (d, 1H, 9.2 Hz, **3**), 7.07 (dd, 1H, 8.4 Hz, **6**), 7.23 (td, 1H, 7.5 Hz, **14**), 7.29 (dd, 2H, 8.4 Hz, **12**, **16**), 7.46 (dd, 2H, 7.1 Hz, **13**, **15**), 7.65 (dd, 1H, 8.1 Hz, **7**), 7.76 (d, 1H, 9.2 Hz, **5**), 7.88 (d, 1H, 8.6 Hz, **4**), 7.93 (d, 1H, 8.6 Hz, **8**), 9.08 (s, 1H, $^3J_{Pt-H}$ = 79.2 Hz, Pt–N=CH). $^{13}C\{^1H\}$ NMR: (CD_2Cl_2) δ 26.0 (**23**), 28.7 (**19**), 30.1 (**20**), 31.9 (**24**), 68.1 (**17**), 73.8 (**18**), 85.3 (**21**, **22**), 110.6 (**1**), 119.5 (**8**), 123.3 (**6**), 123.3 (**12**, **16**), 125.9 (**14**), 128.0 (**7**), 128.2 (**9**), 129.2 (**5**), 129.8 (**13**, **15**), 132.3 (**10**), 136.5 (**4**), 137.6 (**11**), 150.2 (**3**), 157.5 (**#**), 169.3 (**2**).

***4c**-minor isomer.* ^{1}H NMR (CD_2Cl_2, 399.8 MHz, 293 K): 9.24 (s, 1H, $^3J_{Pt-H}$ = 25.2 Hz, Pt–N=CH).

LIFDI-MS, *m*/*z* 549.13 (calculated for $C_{25}H_{24}NOPt$ [M]–OH = 549.15); elemental analysis: for $C_{25}H_{25}NO_2Pt$ Calc. C 53.00; H 4.45; N 2.47; rest 40.08% Found C 53.19; H 4.48; N 2.72; rest 39.61% IR (KBr)/cm^{-1} 1620 (C=N), 3498 (O–H), 1261 (C–O phenolic).

Synthesis of 4d. Dibromo(1,5-cyclooctadiene)platinum(II) (50 mg, 0.108 mmol), *N*-(2-hydroxy-1-naphthalidene)-*p*-chloroaniline (30 mg, 0.11 mmol) and sodium *tert*-butoxide (24 mg, 0.22 mmol) were stirred in THF (30 ml). The reaction mixture was left in a Schlenk tube under nitrogen and stirring overnight. The solution was then filtered under nitrogen, and dried under vacuum for 4 hours. The complex **4d** was obtained as yellow crystals (70 mg, 0.13 mmol, 60% yield).

***4d**-major isomer.* ^{1}H NMR (CD_2Cl_2, 399.8 MHz, 293 K): δ_H 1.71 (m, 1H), 2.18 (m, 2H), 2.61 (m, 2H), 2.90 (m, 1H), 3.80 (m, 1H), 4.05 (m, 1H), 4.98 (m, 2H, **21** and **22**), 6.91 (d, 1H, 9.3 Hz, **3**), 7.03 (dd, 1H, 8.6 Hz, **6**), 7.25 (dd, 2H, 8.6 Hz, **12**, **16**), 7.44 (dd, 2H, 8.9 Hz, **13**, **15**), 7.65 (dd, 1H, 8.1 Hz, **7**), 7.77 (d, 1H, 9.4 Hz, **5**), 7.86 (d, 1H, 8.5 Hz, **4**), 7.91 (dd, 1H, 9.1 Hz, **8**), 9.03 (s, 1H, $^3J_{Pt-H}$ = 69.4 Hz, Pt–N=CH). $^{13}C\{^1H\}$ NMR: (CD_2Cl_2) δ 27.6 (**24**), 28.4 (**23**), 31.3 (**19**), 33.8 (**20**), 68.2 (**17**), 73.8 (**18**), 85.6 (**21**, **22**), 110.2 (**1**), 119.5 (**8**), 123.1 (**3**), 123.1 (**6**), 125.1 (**13**, **15**), 126.0 (**12**, **16**), 126.4 (**9**), 127.3 (**14**), 128.0 (**7**), 129.2 (**5**), 132.3 (**10**), 136.7 (**4**), 137.6 (**11**), 157.6 (**#**), 169.4 (**2**).

***4d**-minor isomer.* ^{1}H NMR (CD_2Cl_2, 399.8 MHz, 293 K): 9.21 (s, 1H, $^3J_{Pt-H}$ = 20.8 Hz, Pt–N=CH).

ESI-MS, positive ion, *m*/*z* 584.1181 (calculated for $C_{25}H_{23}ClNOPt$ [M]–OH = 584.1191, Δ = 0.7 mDa). Elemental analysis: for $C_{25}H_{24}NO_2ClPt$ Calc. C 49.96; H 4.03; N 2.33; rest 43.68% Found C 50.08; H 4.08; N 2.42; rest 43.42%; IR (KBr)/cm^{-1} 1580 (C=N), 3473 (O–H), 1261 (C–O phenolic).

Synthesis of 4e. Dibromo(1,5-cyclooctadiene)platinum(II) (50 mg, 0.11 mmol), *N*-(2-hydroxy-1-naphthalidene)-*p*-methoxyaniline (30 mg, 0.11 mmol) and sodium *tert*-butoxide (24 mg, 22 mmol) in THF (30 ml). The reaction mixture was left in a Schlenk tube under nitrogen and stirring overnight. The solution was then filtered under nitrogen, and dried under vacuum for 4 hours. Complex **4e** was obtained as yellow crystals (70 mg, 0.13 mmol, 60% yield).

***4e**-major isomer.* ^{1}H NMR (CD_2Cl_2, 399.8 MHz, 293 K): δ_H 1.81 (m, 1H), 2.15 (m, 2H), 2.60 (m, 2H), 2.90 (m, 2H), 3.84 (s, 3H, **27**), 4.05 (m, 1H), 4.98 (m, 2H, **21** and **22**), 6.91 (d, 1H, 9.4 Hz, **3**), 7.03 (dd, 1H, 8.5 Hz, **6**), 7.25 (dd, 2H, 8.6 Hz, **12**, **16**), 7.44 (dd, 2H, 8.9 Hz, **13**, **15**), 7.65 (dd, 1H, 8.1 Hz, **7**), 7.77 (d, 1H, 9.3 Hz, **5**), 7.86 (d, 1H, 8.5 Hz, **4**), 7.91 (d, 1H, 8.9 Hz, **8**), 9.06 (s, 1H, $^3J_{Pt-H}$ = 78.4

Hz, Pt-N=CH). $^{13}C\{^{1}H\}$ NMR: (CD_2Cl_2) δ 26.0 (**19**), 27.3 (**20**), 28.6 (**23**), 31.2 (**24**), 55.9 (**27**), 68.2 (**17**), 73.9 (**18**), 84.8 (**21**, **22**), 109.3 (**1**), 114.0 (**12**, **16**), 119.6 (**8**), 122.1 (**3**), 123.0 (**12**), 123.8 (**6**), 124.4 (**9**), 124.5 (**13**, **15**), 128.1 (**7**), 129.4 (**5**), 136.0 (**10**), 137.1 (**4**), 147.4 (**11**), 157.9 (**#**), 158.4 (**14**), 169.0 (**2**).

***4e**-minor isomer.* ^{1}H NMR (CD_2Cl_2, 399.8 MHz, 293 K): 9.24 (s, 1H, $^{3}J_{Pt-H}$ = 23.6 Hz, Pt–N=CH).

LIFDI-MS, *m*/*z* 579.16 (calculated for $C_{26}H_{26}NO_2Pt$ [M]–OH = 579.16). Elemental analysis: for $C_{26}H_{27}NO_3Pt$ Calc. C 52.35; H 4.56; N 2.35; rest 40.74% Found C 52.46; H 4.59; N 2.54; rest 40.41% IR (KBr)/cm^{-1} 1580 (C=N), 3458 (O–H), 1256 (C–O phenolic), 1428 (C–O ether aromatic).

General method for the hydrogenative and dehydrogenative silylation of alkenes

Reaction with styrene. The appropriate complex **4**, (5 mol%) was dissolved in d^8-toluene (0.5 ml) and removed from the glove-box. $HSiEt_3$ (0.18 mmol, 27 μl) and styrene (0.18 mmol, 20 μl) were added in a 1 : 1 molar ratio. The reaction mixture was kept at the stated temperature for 12 hours. The reactions were performed in a range of different temperatures going from 50 °C, 70 °C, 90 °C and 110 °C. The conversion to products and the ratio of the product isomers was determined by integration of the ^{1}H NMR spectra, and confirmed by GC-MS.

Notes and references

1 (*a*) P. Guerriero, S. Tamburini and P. A. Vigato, *Coord. Chem. Rev.*, 1995, **139**, 17; (*b*) P. A. Vigato and S. Tamburini, *Coord. Chem. Rev.*, 2004, **248**, 1717; (*c*) A. D. Garnovskii, A. L. Nivorozhkin and V. I. Minkin, *Coord. Chem. Rev.*, 1993, **126**, 1; (*d*) R. Ziessel, *Coord. Chem. Rev.*, 2001, **216–217**, 195.

2 (*a*) J.-J. Zhang, H.-J. Zhou and A. Lachgar, *Angew. Chem., Int. Ed.*, 2007, **46**, 4995; (*b*) B. Kaitner, E. Mestrovic and G. Pavlovic, *J. Chem. Crystallogr.*, 1998, **28**, 77; (*c*) A. Blagus and B. Kaitner, *Acta Crystallogr., Sect. C: Cryst. Struct. Commun.*, 2009, **C65**, m455; (*d*) H.-D. Bian, X.-E. Yang, Q. Yu, Z.-L. Chen, H. Liang, S.-P. Yan and D.-Z. Liao, *J. Mol. Struct.*, 2008, **872**, 40; (*e*) W.-X. Zhang, C.-Q. Ma and S.-F. Si, *Transition Met. Chem.*, 2001, **26**, 380; (*f*) M. Dey, C. P. Rao, P. K. Saarenketo and K. Rissanen, *Inorg. Chem. Commun.*, 2002, **5**, 924; (*g*) S. M. El-Madani, O. A. M. Ali and R. M. Ramadan, *J. Mol. Struct.*, 2005, **738**, 171; (*h*) M. Hosseini, S. F. L. Mertens, M. Ghorbani and M. R. Arshadi, *Mater. Chem. Phys.*, 2003, **78**, 800; (*i*) M.-L. Tong, X.-M. Chen, B.-H. Ye and L. N. Ji, *Angew. Chem., Int. Ed.*, 1999, **38**, 2237.

3 (*a*) M. S. Sigman and E. N. Jacobsen, *J. Am. Chem. Soc.*, 1998, **120**, 4901; (*b*) P. G. Cozzi, *Chem. Soc. Rev.*, 2004, **33**, 410; (*c*) B. N. Shelimov, *Ross. Khim. Zh.*, 2000, **44**, 57; (*d*) K. C. Gupta and A. K. Sutar, *Coord. Chem. Rev.*, 2008, **252**, 1420; (*e*) T. Katsuki, *Chem. Soc. Rev.*, 2004, **33**, 437; (*f*) P. G. Gozzi, *Chem. Soc. Rev.*, 2004, **33**, 410; (*g*) F. Blank and C. Janiak, *Coord. Chem. Rev.*, 2009, **253**, 827.

4 Y. J. Hamada, *IEEE Trans. Electron Devices*, 1997, **44**, 1208.

5 (*a*) F. Faridbod, M. R. Ganjali, R. Dinarvand, P. Norouzi and S. Riahi, *Sensors*, 2008, **8**, 1645; (*b*) H.-C. Wu, P. Thanasekaran, C.-H. Tsai, J.-Y. Wu, S.-M. Huang, Y.-S. Wen and K.-L. Lu, *Inorg. Chem.*, 2006, **45**, 295; (*c*) C. Lordeiro and F. Pina, *Coord. Chem. Rev.*, 2009, **253**, 1353; (*d*) S. Khatua, S. H. Chol, J. Lee, J. O. Huh, Y. Do and D. G. Churchlll, *Inorg. Chem.*, 2009, **48**, 1799.

6 (*a*) A. K. Sutar, Y. Das, S. Pattnaik, N. Nath, P. Rath and T. Maharana, *Int. J. Mater. Sci. Appl.*, 2013, **2**, 136; (*b*) P. G. Cozzi, L. S. Dolci, A. Garelli, M. Montalti, L. Prodi and N. Zaccheroni, *New J. Chem.*, 2003, **27**, 692; (*c*) A. V. Metelitsa, A. S. Burlov, S. O. Bezuglii, I. G. Borodkina, V. A. Bren, A. D. Garnovskii and V. I. Minkin, *Russ. J. Coord. Chem.*, 2006, **32**, 858.

7 (*a*) A. Garoufis, S. K. Hadjikakou and N. Hadjiliadis, *Coord. Chem. Rev.*, 2009, **253**, 1384; (*b*) H. Q. Chen, S. Hall, B. Zheng and J. Rhodes, *BioDrugs*, 1997, **7**, 217; (*c*) R. Ramesh and M. Sivagamasundari, *Synth. React. Inorg. Met.-Org. Chem.*, 2003, **33**, 899.

8 (*a*) A. Sasmal, E. Garribba, C. J. Gómez-García, C. Desplanches and S. Mitra, *Dalton Trans.*, 2014, **43**, 15958; (*b*) M. Padmaja, J. Pragathi and C. G. Kumari, *J. Chem. Pharm. Res.*, 2011, **3**, 602.

9 (*a*) B. De Clercq and F. Verpoort, *Adv. Synth. Catal.*, 2002, **344**, 639; (*b*) C. Janiak, A. C. Chamayou, A. K. M. Royhan Uddin, M. Uddin, K. S. Hagen and M. Enamullah, *Dalton Trans.*, 2009, 3698.

10 (*a*) S. S. Djebbar, B. O. Benali and J. P. Deloume, *Transition Met. Chem.*, 1998, **23**, 443; (*b*) M. H. Lee, T. V. Giap, S. H. Kim, Y. H. Lee, C. Kang and J. S. Kim, *Chem. Commun.*, 2010, **46**, 1407.

11 S. R. Salman, S. H. Shawkat and F. S. Kamounah, *Can. J. Appl. Spectrosc.*, 1992, **37**, 46.

12 F. S. Kamounah and S. R. Salman, *Spectrosc. Lett.*, 1996, **29**, 659.

13 L. Antonov, M. F. Fabian, D. Nedeltcheva and F. S. Kamounah, *J. Chem. Soc., Perkin Trans. 2*, 2000, 1173.

14 B. M. Draškovic, G. A. Bogdanović, M. A. Neelakantan, A.-C. Chamayou, S. Thalamuthu, Y. S. Avadhut, J. S. auf der Günne, S. Banerjee and C. Janiak, *Cryst. Growth Des.*, 2010, **4**, 1665.

15 Z. Rozwadowski, W. Schilf and B. Kamienski, *Magn. Reson. Chem.*, 2005, **43**, 573.

16 (*a*) B. F. G. Johnson, J. Lewis and M. S. Subramanian, *Chem. Commun.*, 1966, 117; (*b*) H. Takahashi and J. Tsuji, *J. Am. Chem. Soc.*, 1968, **90**, 2387; (*c*) B. F. G. Johnson, J. Lewis and M. S. Subramanian, *J. Chem. Soc. A*, 1968, **8**, 1993; (*d*) G. R. Hoel, R. A. Stockland, G. K. Anderson, F. T. Ladipo, J. Braddock-Wilking, N. P. Rath and J. C. Mareque-Rivas, *Organometallics*, 1998, **17**, 1155; (*e*) J. Vicente, M. T. Chicote, C. MacBeath, J. Fernández-Baeza and D. Bautista, *Organometallics*, 1999, **18**, 2677.

17 E. Guiu, C. Claver and S. Castillón, *J. Organomet. Chem.*, 2004, **689**, 1911.

18 (*a*) J. L. Speier, J. A. Webster and G. H. Barnes, *J. Am. Chem. Soc.*, 1957, **79**, 974; (*b*) J. L. Speier, in *Adv. Organomet. Chem.*, ed. F. G. A. Stone and R. West, Academic Press, New York, 1979, vol. 17, pp. 407–447.
19 (*a*) B. J. Truscott, A. M. Z. Slawin and S. P. Nolan, *Dalton Trans.*, 2013, **42**, 270; (*b*) D. Troegel and J. Stohrer, *Coord. Chem. Rev.*, 2011, **255**, 1440.
20 B. Marciniec, *Advances In Silicon Science*, 2009, **1**, 3–51.
21 A reaction with 2 mol% catalyst was unsuccessful.
22 D. Marquardt, J. Barthel, M. Braun, C. Gantera and C. Janiak, *CrystEngComm*, 2012, **14**, 7607.
23 O. V. Dolomanov, L. J. Bourhis, R. J. Gildea, J. A. K. Howard and H. Puschmann, *J. Appl. Crystallogr.*, 2009, **42**, 339.
24 L. Palatinus and G. Chapuis, *J. Appl. Crystallogr.*, 2007, **40**, 786; L. Palatinus and A. Van der Lee, *J. Appl. Crystallogr.*, 2008, **41**, 975; L. Palatinus, S. J. Prathapa and S. Van Smaalen, *J. Appl. Crystallogr.*, 2012, **45**, 575.
25 G. M. Sheldrick, *Acta Crystallogr., Sect. A: Fundam. Crystallogr.*, 2008, **64**, 112.
26 R. J. Angelici, *Inorg. Synth.*, 1990, **28**, 347.

